



SLIDING-BLOCK BACK ANALYSES OF LIQUEFACTION-INDUCED SLIDES

Constantine A. STAMATOPOULOS¹ and Stavros ANEROUSSIS,¹

SUMMARY

Sliding system models where the slide consists of parts sliding in different inclinations have been proposed (Stamatopoulos et al, 2000, Sarma and Chlimitzas, 2000). These models simulate changes of geometry of the soil mass with the distance moved towards a gentler configuration, that greatly affect the seismic displacement when this displacement is large.

The two-body model that was proposed by Stamatopoulos et al (2000), even simplified simulates with reasonable accuracy the displacement of both the upper and the lower part of liquefaction-induced slides of small dams and embankments. Yet, the Stamatopoulos et al (2000) model assumes only cohesion resistance. It is applicable when the undrained soil strength is mobilized everywhere. In cases of earthquake-induced failures of dams and embankments, often the lower part of the slip surface is below the water level, and liquefies, but the upper part is above the water table and does not liquify.

In the paper, the Stamatopoulos et al (2000) sliding system model is extended to include both frictional and cohesion components of resistance in order to be able to simulate the slides described above. Then, the modified model is used to back-estimate the residual shear strength of four slides of small dams and embankments. Finally, the correlation of the residual soil strength and the blow count resistance of the SPT of these cases is compared to the relationships that have been proposed by Seed and Harder (1990) and Ishihara (1993).

1. INTRODUCTION

During recent earthquakes, small dams and embankments were badly damaged as a result of earthquakes (e.g. Stamatopoulos, 2003). The excessive deformation of these earth structures was a result of liquefaction within the earth structures, or at the top of the underlain soil. Some of these case studies are well-documented: the initial and deformed geometries have been recorded, and field standard penetration tests were performed. Characteristics of the applied earthquake are also known.

¹ Stamatopoulos and Associates Co., 5 Isavron street, Athens 114-71, Greece,
e-mail: kostama@athena.compulink.gr

Analysis of such slides provides a unique opportunity to correlate the blow count resistance of the Standard Penetration Test (SPT) to the residual strength of a liquefied soil. Evaluation of the residual strength of a liquefied soil is one of the most difficult problems in contemporary geotechnical engineering practice, mainly because it is difficult to obtain undisturbed samples in sands. Approaches have been developed to relate the shear strength of liquefied soils to the SPT blow count resistance: Seed and Harder (1990) give a range of the shear strength of liquefied soils, c_u , while Ishihara (1993) gives a lower bound of the ratio of the shear strength and the consolidation vertical stress c_u/σ'_v in terms of the corrected blow count of the SPT.

The relations of Seed and Harder (1990) and Ishihara (1993) are probably based on stability analyses of the initial and final slide configurations assuming a safety factor equal to 1, and/or analyses using the sliding-block model (Newmark, 1965). However, the factor of safety exactly before the slide is less than one because motion develops; after the slide it is greater than one, as a result of inertia. In addition, the conventional sliding-block model has shortcomings in back-estimating the soil strength of earthquake-induced slides when seismic displacement is large. The reason is that the change on geometry of the sliding mass, that greatly affects the seismic displacement, is not modeled.

To overcome the above problems, sliding system models, where the slide consists of parts sliding in different inclinations have been proposed (Stamatopoulos et al, 2000, Sarma and Chlimitzas, 2000). The model by Stamatopoulos et al (2000) consists of two sliding bodies, while the model of Sarma and Chlimitzas (2000) of "n" sliding bodies. For soil to move along the (external) lines with different inclinations, internal shearing must be allowed along lines intersecting the angle between the external lines. This internal sub-plane(s) together with the external sub-planes define the bodies of these sliding system models. Mass of the upper bodies is transferred to the lower bodies as the sliding system moves downwards. The stress state along the internal lines must be at failure (Sarma, 1979).

The 2-body model by Stamatopoulos et al (2000) has been used to analyze dam slides triggered by the 1971 San Fernando earthquake and by the 1985 Chilean earthquake (Stamatopoulos et al, 2000) and the seismic displacement of the mole embankment at King Harbor Redondo Beach as a result of the Northridge earthquake of 1994 (Stamatopoulos and Aneroussis, 2004). These analyses have illustrated that this sliding system model, even simplified, simulates with reasonable accuracy the displacement of both the upper and the lower part of the slides. Yet, further study of case histories of earthquake-induced slides of a number of slides of dams and embankments has illustrated that in many cases the lower sub-plane is below the water level and liquefies, but the upper part is mainly above the water table and/or does not liquify. The Stamatopoulos et al (2000) model assumes only cohesion resistance at both the external sub-planes and the internal sub-plane. It is applicable when the undrained soil strength is mobilized at both the upper and lower sub-planes by using the undrained soil strength in place of the resistance. Thus, it cannot be used for the case described above.

It is inferred that a practical sliding system model that simulates with reasonable accuracy the seismic displacement of the slides described above is the two-body model that includes both frictional and cohesion components of resistance. In the present paper such a model is formulated. Then, it is used to back-estimate the residual shear strength of four slides of small dams and embankments. Finally, the correlation of the residual soil strength and the blow count resistance of the SPT is compared to the relationships that have been proposed by Seed and Harder (1990) and Ishihara (1993).

2. THE MODEL

General

The 2-dimensional mass sliding as a result of a horizontal earthquake on two sub-planes, shown in Fig. 1, is considered. An internal sub-plane separates the two bodies. Thus, two bodies can be defined sliding in two inclinations: body 1 sliding at the gentler inclination and body 2 at the steeper. The shape of the top (ground) surface of body 2 can be defined with successive segments and this is necessary because these geometric particularities affect the mass transfer between the two bodies. Yet, as in the cases histories that will be studied, the top of the part of body 2 that changes inclination consists of only one segment, only the inclination of this first segment will be specified.

The parameters that define the model and affect the solution can be separated into (a) the inclinations of the two external and the internal sub-planes, (b) the initial masses and weights of the two bodies, (c) other factors of the initial geometry, (d) the resistance along the external and internal slip sub-planes and (e) the total and effective unit weights of the mass that changes inclination, γ_t and γ_b . Specifically referring to Figs 1 and 2, we must define (a) the inclinations of the external sub-planes where the two bodies slide, α_1 and α_2 , and the inclination of the internal sub-plane, $90^\circ - \delta_2$, (b) the initial masses and weights of the two bodies m_{10} , m_{20} and W_{10} , W_{20} , (c) the initial contact lengths, b_{10} and b_{20} , the initial length of the internal sub-plane, d_0 , and the inclination of the first segment of the top body 2 relative to α_2 , θ , (d) the frictional and cohesive resistance along the external and internal sub-planes, ϕ_1 , ϕ_2 , ϕ'_2 and c_1 , c_2 , c'_2 , where the tone corresponds to the internal sub-plane and (e) the total and effective unit weights of the mass changing inclination, γ_t and γ_b . Finally, the distances moved along the first and second slip sub-planes are defined as u_1 and u_2 respectively.

The proposed model assumes that the angle of the internal sub-plane of the slide, δ_2 , is constant and does not change as a function of the distance moved. In addition, the 2-dimensional total mass of the slope is taken to be constant throughout the sliding period. Thus, at each time increment the incremental change in cross-sectional area of body 1 should equal the change of area of body 2, or,

$$d(t) du_1(t) \sin(90^\circ + \delta_2 + \alpha_1) = d(t) du_2(t) \sin(90^\circ + \delta_2 + \alpha_2) \quad (1a)$$

where d indicates incremental change and (t) denotes function of time. This gives that:

$$u_1 / u_2 = du_1 / du_2 = \cos(\delta_2 + \alpha_2) / \cos(\delta_2 + \alpha_1) = \lambda_1 \quad (1b)$$

or, that the ratio of displacements moved along the two slip lines depends only on the relative inclinations of the external slip lines and the line of internal shearing.

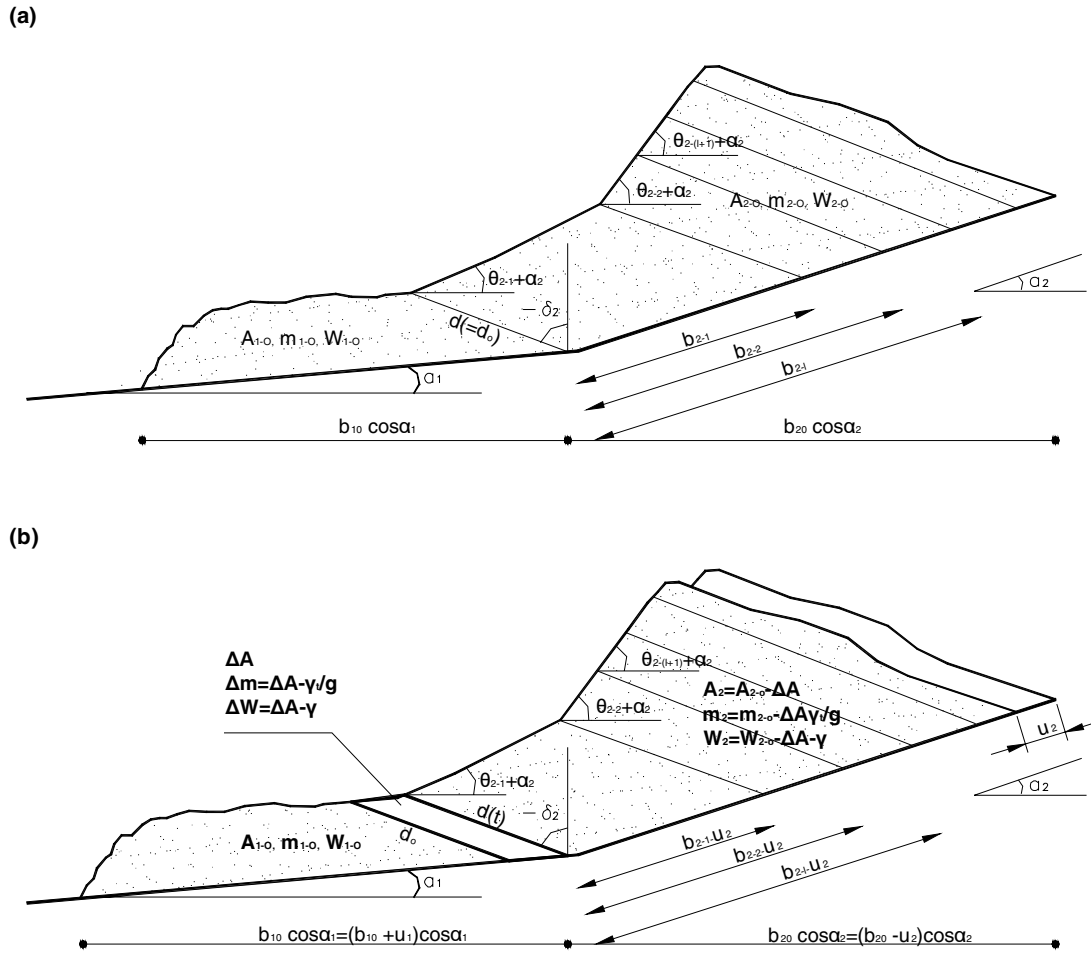


Fig. 1. Sliding system considered : (a) Initial position, (b) position when the distance moved by the second body is u_2 (Note that $u_2 < b_{2-1}$).

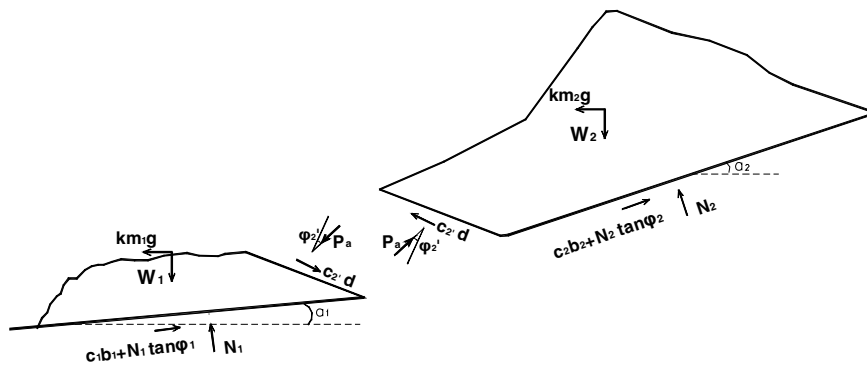


Fig. 2. Forces on bodies 1 and 2: (a) Body 1, (b) Body 2.

The governing equation of motion.

Fig. 2 gives the exerted forces in the two bodies. The equation of motion of body 1 in the direction of sliding is:

$$m_1(d^2u_1/dt^2) = \frac{1}{\cos \phi_1} \cdot [m_1 g \sin(\alpha_1 - \phi_1) + P_a \cos(\phi'_2 + \phi_1 - \alpha_1 - \delta_2) - c_1 b_1 \cos \phi_1 - c'_2 d \sin(\phi_1 - \delta_2 - \alpha_1) + kW_1 \cos(\alpha_1 - \phi_1)] \quad (2a)$$

where g is the acceleration of gravity, $\{g k\}$ is the applied acceleration and the other parameters were defined previously. Note that the weight W_1 is not always equal to the product $\{m_1 g\}$, since in the case of submerged mass, it corresponds to the buoyant weight. Similarly, the equation of motion of body 2 in the sliding direction is:

$$m_2(d^2u_2/dt^2) = \frac{1}{\cos \phi_2} \cdot [m_2 g \sin(\alpha_2 - \phi_2) - P_a \cos(\phi'_2 + \phi_2 - \alpha_2 - \delta_2) - c_2 b_2 \cos \phi_2 + c'_2 d \sin(\phi_2 - \delta_2 - \alpha_2) + kW_2 \cos(\alpha_2 - \phi_2)] \quad (2b)$$

Combination of the above equations, and using equation (1) relating the incremental distance moved by the two bodies, gives that the governing equation of the sliding system is:

$$(d^2u_1/dt^2) = Z_1 g (k(t) - k_c) \quad (3a)$$

where,

$$Z_1 = \frac{m_1 \cos(\alpha_1 - \phi_1) + \frac{m_2 \cos(\alpha_2 - \phi_2)}{\mu_1}}{m_1 \cos \phi_1 + \frac{m_2 \cos \phi_2}{\lambda_1 \mu_1}} \quad (3b)$$

$$k_c = \frac{AA}{BB} \quad \text{with} \quad (3c)$$

$$AA = W_1 \sin(\phi_1 - \alpha_1) + c_1 b_1 \cos \phi_1 + c'_2 d_2 \sin(\phi_1 - \delta_2 - \alpha_1) + (W_2 \sin(\phi_2 - \alpha_2) + c_2 b_2 \cos \phi_2 - c'_2 d_2 \sin(\phi_2 - \delta_2 - \alpha_2)) / \mu_1 \quad (3d)$$

$$BB = m_1 \sin(\alpha_1 - \phi_1) + \frac{m_2 \sin(\alpha_2 - \phi_2)}{\mu_1} \quad (3e)$$

where

$$\mu_1 = \cos(\phi'_2 + \phi_2 - \delta_2 - \alpha_2) / \cos(\phi'_2 + \phi_1 - \delta_2 + \alpha_1) \quad (3f)$$

The change of the lengths, masses and weights

To solve equation (3), we need to express b_1 , b_2 , W_1 , W_2 , m_1 , m_2 , d , as a function of the distance moved, u_1 . The change of the lengths and cross-sectional area of the second body is

$$b_2 = b_{20} - u_1 / \lambda_1 \quad (4)$$

$$d_2 = d_{20} + \frac{\sin \theta_2}{\cos(\theta_2 + \alpha_2 + \delta_2)} \cdot u_2 = d_{20} + \frac{\sin \theta_2}{\cos(\theta_2 + \alpha_2 + \delta_2)} \cdot \frac{u_1}{\lambda_1} \quad (5)$$

$$\Delta A_2 = d_{20} \cdot \cos(\alpha_2 + \delta_2) \cdot \frac{u_1}{\lambda_1} + \frac{0.5 \cdot \cos(\alpha_2 + \delta_2) \cdot \sin \theta_2}{\cos(\theta_2 + \alpha_2 + \delta_2)} \cdot \left(\frac{u_1}{\lambda_1} \right)^2 \quad (6)$$

For the slides that will be considered in the present work, the lower slip sub-plane is about horizontal. Thus, there is room in order the lower slip sub-plane to increase by u_1 . It is inferred that the change of length and cross-sectional area of the first body are

$$b_1 = b_{10} + u_1 \quad \Delta A_1 = -\Delta A_2 \quad (7)$$

Finally, the changes in masses and weights of the two bodies is

$$\Delta W_i = \Delta A_i \gamma \quad \Delta m_i = \Delta A_i \gamma_t / g \quad (8)$$

where i takes the values of 1 and 2 and $\gamma = \gamma_b$ below the water table line and $\gamma = \gamma_t$ above the water table line.

Discussion

A computer program using the language fortran solving numerically the above equations was written. This computer program is used in the analyses below.

The model is recommended only for back analyses of slides. In such cases the model parameter δ_2 can be obtained from the distance moved along the two slip sub-planes and the compatibility condition (1b). At this point it can be noted that according to the theory of limit equilibrium, the angle δ_2 corresponds to that giving the minimum value of the critical acceleration, k_c (Sarma, 1979). In addition, δ_2 does not necessarily have to be constant: as the body slides the relative masses of the two bodies change and the inclination of the interslice line producing a minimum critical acceleration can change. It is beyond the scope of the paper to simulate these effects on the value of δ_2 , which is taken as being constant during the mass movement. As a check, in the case studies given later, the angle δ_2 obtained from the distance moved is compared with that obtained from the limit equilibrium condition at the initial slide configuration.

3. SLIDES THAT WILL BE BACK-ANALYZED

Four well-defined 2-dimensional slides, where a large part of the slope is above the water table line, but the lower part of the slip surface is submerged were found in the literature. Their cross-sections are given in Fig 3. They are described below.

La Marquesa Downstream and La Palma Dam Slides (De Alba et al, 1988)

La Marquesa Dam and La Palma Dam were subjected to large ground accelerations by the Chilean earthquake of March 3, 1985, that had a surface wave magnitude M_s of 7.8. La Marquesa Dam was located 45 km from the earthquake epicenter and the peak acceleration on site was estimated around 0.6g. La Palma Dam was located 75 km from the earthquake epicenter and the peak acceleration in the vicinity of the dam reached 0.46g.

Major sliding of both the upstream and downstream slopes of the La Marquesa Dam took place (Fig. 3a). The maximum horizontal displacement measured at the downstream slope was about 5m. There also was a 2 m loss of freeboard and extensive longitudinal cracking. The average measured post-earthquake

equivalent clean sand value of the SPT, $N_{1(60)}$, of the silty sand layer of the downstream slope that liquefied was 9 (De Alba et al., 1988).

Major sliding of the upstream slope of La Palma Dam also occurred (Fig. 3b). The maximum horizontal displacement measured was 5m. In addition, considerable longitudinal cracking was observed. The average measured post-earthquake equivalent clean sand values of $N_{1(60)}$ of the silty sand layer that liquefied was 3 (De Alba et al., 1988).

Embankment of Kushiro river (Kaneko et al, 1995)

The Kushiro-Oki Earthquake of magnitude 7.8 occurred in Hokkaido, the northern island of Japan, on January 15, 1993. Along the Kushiro River on alluvial lowlands, dikes were given deadly blows in a long extent, while the peripheral surface (marsh and farmland) showed neither conspicuous breakage nor sand eruption. A peat bed of 3 to 6 m thickness spreads over alluvial lowlands of the Kushiro River. The peat bed was underlain by a sand bed and a thick soft marine clay bed. River levee with its height of 5 to 7 m had sank 2 to 3m into the peaty bed prior to the earthquake. Materials of the levee are generally sandy soil originated from volcanic ashes. Dike material below the ground surface was submerged under ground water and was potentially liquefiable.

Fig. 3c shows a sketch of failure of the Kushiro River dike. The failures are caused by liquefaction of dike materials sank into peat bed. The average SPT N value of the dike material under water table was 5. Peak accelerations were estimated as approximately 0.35g.

Embankment of Rinnio river (Tika and Pitilakis, 1999)

The Kozani-Grevena earthquake of magnitude 6.0 occurred on May 13, 1995, in North-Western Greece. The most impressive geotechnical damage observed was the failure of the Rinnio bridge embankment.

During the earthquake, the embankment suffered serious damage. The pavement to a great length settled by 1 to 2 m, while according to a survey carried out after the earthquake, the maximum horizontal displacement was of the order of 0.8 to 2 m, depending on the location (Fig. 3d).

An extensive geotechnical investigation was carried out after the earthquake. The geotechnical investigation showed that the embankment is constructed from compacted clayey-sandy gravel and it is founded on a 3.5 to 4 m thick layer of loose silty sand, which extends beyond the embankment toe. Then follows a 7.5 m thick layer of dense sandy gravel and cobbles and a layer of marly clay. The latter extends to the bedrock with an increasing stiffness.

The minimum number of SPT blows measured at the silty sand layer ten days after the earthquake was $N_{SPT} = 18$. The corresponding $(N_1)_{60}$ value equals to 14. Also, the piezometric ground water table at the silty sand layer at the same date was 4 m above the pavement, indicating the existence of a significant yet undissipated excess pore water pressure. Surficial effects of liquefaction, such as sand boils, were observed. These field observations indicated that failure was induced by the liquefaction of the silty sand layer. Furthermore, the maximum applied acceleration during the earthquake outside the region that liquified was about 0.27g.

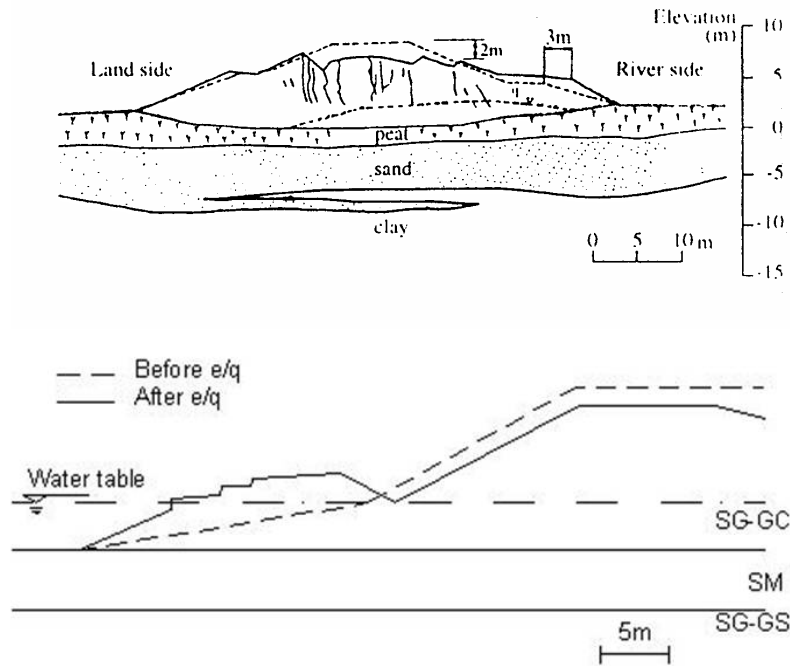
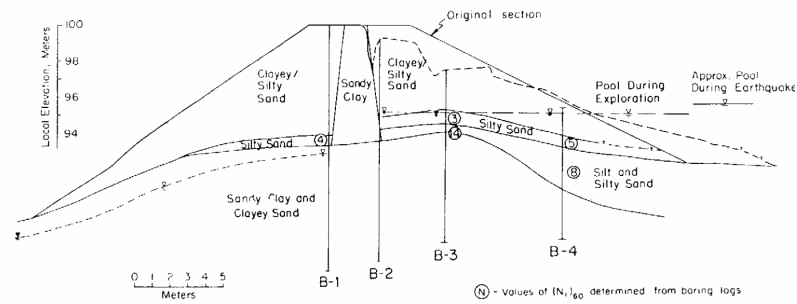
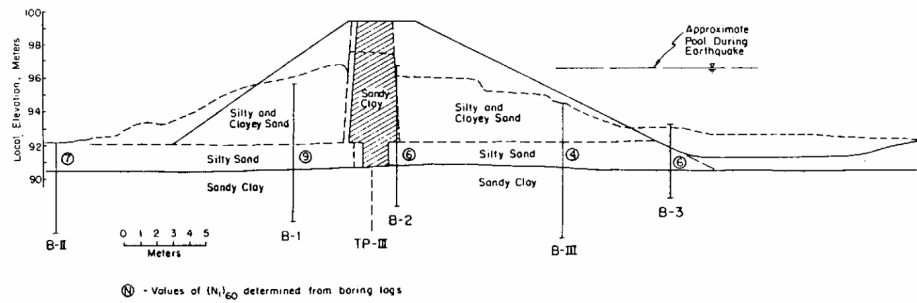


Fig. 3. The slides studied in the present work: (a) the downstream slope of the La Marquesa Dam (De Alba et al, 1988), (b) the La Palma Dam (De Alba et al, 1988), (c) the embankment of Kushiro river (Kaneko et al, 1995) and (d) the embankment of Rinnio river (Tika and Pitilakis, 1999).

Undrained monotonic triaxial test (CU) on the silty sand gave for consolidation stress $\sigma'_c = 114 \text{ kPa}$, an undrained residual strength c_{us} of 26.2 to 33.1 kPa; the corresponding ratio c_{us}/σ'_v , where σ'_v is the vertical stress perpendicular to the slip surface prior to shearing, equals to 0.149 to 0.188, assuming that the sand is normally-consolidated.

4. BACK-ANALYSES

Model Geometries

The methodology that was used to select the model geometries simulating the slides described above was the following:

- The lower slip sub-plane was taken on the base of the embankments with inclination consistent to the failure mechanism. The location and inclination of the upper slip sub-plane was estimated based on the theory of limit equilibrium, as the sub-plane that corresponds to the minimum value of the critical acceleration. No data exists on the unit weight of the soil. A reasonable assumption, used in the analysis, is that the total unit weight of the soil, γ_t , equals to 2 t/m^3 .
- In order to finalize the model geometry, the inclination of the internal slip surface must be determined. This inclination was determined based on the ratio of the measured displacement of the upper and lower external sub-planes, using equation (1b), as given in table 1.

Based on all of the above, Fig 4 gives the initial geometry of the model slides. In addition, all the parameters (except those of the soil strength) defining the model slides are given in Table 2.

Results

In sliding-block analyses the applied acceleration corresponds to the average acceleration along the slip surface (e.g. Kramer, 1996). The peak horizontal acceleration that has been measured, or estimated, at, or near, the slip surface by the scientists who studied the slides, are given in table 3.

Different accelerograms, normalized at the maximum accelerations of table 1, were applied to investigate the effect of the applied accelerogram on the back-figured undrained soil strength. The following accelerograms covering a wide range of fundamental period and earthquake magnitude values for possible earthquakes were considered:

- Port Island (Kobe, Japan), 17/1/1995, component East-West at depth 16m., M (=earthquake magnitude)=7.2, R (=distance from the epicenter)= 5 Km, a_m (=maximum value of the acceleration) = 0.35g, T_f (=fundamental period)=0.7 s.
- El-Centro (California, USA), 18/5/1940, component North-South, M = 6.5, R =5 Km, a_m = 0.35g, T_f =0.6 s.
- San Fernando - Avenue of Stars (California, USA), 1971, component East-West, M =6.5, R =40 Km, a_m =0.15g, T_f =0.15 s.
- Kalamata (Greece), 13/9/1986, M =5.75, R =9 Km, Municipality Building, longitudinal component: a_m =0.24g, T_f =0.35s
- Gazli (former USSR), 17/5/1976, M =7.3, a_m =0.70g, T_f =0.1 s.

Above the water table, and/or at the region where liquefaction does not occur, a residual friction angle of 30° and zero cohesive resistance is assumed for the sandy soil. An exception is the Rimnio embankment, where, as the upper part of the slides is partly submerged, to account for generation of excess pore pressures it is assumed that $\phi'_2 = 25^\circ$. Using back analysis, the sand strength c_u of the soil below the water table that corresponds to the measured seismic displacement was estimated.

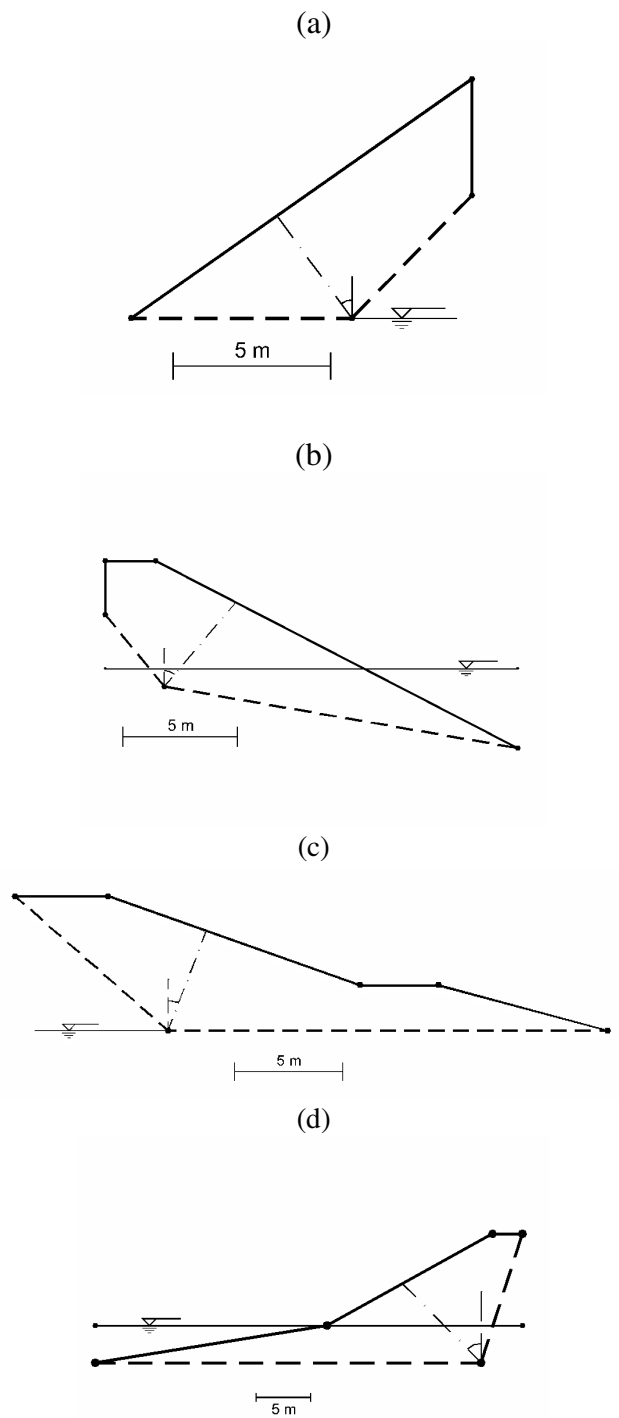


Fig. 4. The simulation of the initial geometries of the slides of Fig 4 with the proposed model: (a) the downstream slope of the La Marquesa Dam, (b) the La Palma Dam, (c) the embankment of Kushiro river and (d) the embankment of Rimnio river.

Thus, the model parameters c_2 and c'_2 are taken zero, while ϕ_2 and ϕ'_2 are taken 30° or 25° . The model parameter c_1 is taken equal to c_u , while ϕ_1 is taken zero. The sand strength c_u was first estimated for the Port Island input motion, as given in table 3. Table 3 also gives the back-estimated values of c_u/σ' for all slides considered. The average vertical stress at the slip sub-plane that liquifies, σ' , was estimated according to Olson et al (2000) as

$$\sigma' = \frac{\sum(l_i \sigma'_i)}{\sum l_i} \quad (9)$$

where l_i is the length of the slip surface where the vertical effective stress equals σ'_i .

The value of the critical acceleration at the initial configuration of the slides predicted in the above analyses is also given in table 3. It can be observed that the large measured slope displacements correspond to negative critical acceleration value. Negative critical acceleration value indicates static instability.

The back-estimated residual soil strength in terms of the applied accelerogram are given in table 4a. It can be observed that the effect of the applied accelerogram on the back-estimated residual soil strength is small, presumably because most of the seismic displacement is a result of static instability (due to earthquake-induced loss of strength).

The effect of the soil strength of the sandy soils above the water table and/or at the region that does not liquify was also investigated. The frictional resistance of the sandy soils above the water table varied from 25° to 35° . The back-estimated residual soil strength, in terms of the soil strength of body 2 is given in table 4b. It can be observed that as the soil strength increases, the back-estimated residual soil strength of body 2 decreases.

Correctness of the analyses

According to the theory of limit equilibrium, the internal sub-plane must correspond to the minimum value of the critical acceleration (Sarma, 1979). Fig 5 gives the critical acceleration in terms of the inclination of the internal sub-plane at the initial slide configuration. The values of soil strength used in the analyses are similar to those back-estimated above. Table 1 gives the angle δ_2 obtained from Fig. 5 according to the limit equilibrium condition. It can be observed that the range of the angles δ_2 , that produce a minimum in the critical acceleration is within about 15° of the value of δ_2 from the ratio u_1/u_2 . The above illustrates the validity of the proposed approach.

As described above, in the case of the Rimnio embankment the undrained soil strength was estimated by triaxial constant-volume tests by Tika and Pitilakis (1999). The measured ratio c_u/σ'_v was 0.15 to 0.19. Based on table 3, the back analysis gave for the case of Rimnio, a c_u/σ' ratio equals to 0.16. Comparing this value with the measured ratio c_u/σ'_v , it can be observed that it agrees.

Table 1. Relative displacement along the two slip sub-planes and corresponding angle δ_2 . The value of critical acceleration based on the analysis of Fig 5 is also given.

Case	u_1	u_2	$\delta_{2\text{-kinematic}}$	$\delta_{2\text{-stability}}$
La Marquesa Dam downstream	5.0	4.0	-35.0	-20.0
La Palma dam	5.0	4.3	-41.0	-30.0
Embankment of Kushiro river	3.0	3.0	-21.0	-25.0
Embankment of Rimnio river	2.0	2.0	-36.0	-25.0

Table 2. The model parameters for each case

Case	α_1, α_2 ($^\circ$)	$m_1 g, m_2 g$ (kPa)	W_1, W_2 (kPa)	b_1, b_2, d (m)	δ_2, θ ($^\circ$)
La Marquesa Dam downstream	0, 45	221.4, 433.4	221.4, 433.4	7.0, 5.4, 4.0	-37, -10
La Palma dam	10, 50	637.0, 359.0	432.1, 353.9	15.6, 4.0, 4.8	-41, -21
Embankment of Kushiro	0, 41	867.8, 500.4	867.8, 500.4	20.3, 9.4, 4.9	-21, -21
Embankment of Rimnio	0, 72	2124.2, 1089.6	1328.4, 1029.2	35.2, 12.4, 9.9	-36, -43

Table 3. The maximum applied horizontal acceleration, and undrained strength that was back-estimated for each case. The corresponding critical acceleration is also given. The Hyogoken-Nambu Quake was applied and a frictional resistance of 30° was assumed for body 2, except for the Rimnio embankment case, where a frictional resistance of 25° was assumed.

Case	a_{\max} (g)	a_{co} (g)	c_u (kPa)	σ'_v (kPa)	c_u / σ_v
La Marquesa Dam downstream	0.60	-0.03	6	60	0.10
La Palma dam	0.45	-0.02	9.2	40	0.23
Embankment of Kushiro river	0.50	-0.01	3.8	50	0.08
Embankment of Rimnio river	0.07	-0.01	14.0	90	0.16

Table 4. Parametric analyses. Effect of the applied accelerogram on the back-estimated residual soil strength

(a) in terms of the applied earthquake

Case	Port Island Quake	El-Centro Quake	San Fernando Quake	Kalamata quake	Gazli quake
La Marquesa Dam downstream	6.0	6.0	6.0	6.0	5.8
La Palma dam	9.2	9.2	9.2	9.2	9.0
Embankment of Kushiro river	3.8	3.5	3.6	3.5	3.7
Embankment of Rimnio river	14.0	13.5	14.0	13.5	14.0

(b) in terms of the frictional resistance above the water table line (Hyogoken-Nambu quake)

Case	$\phi=25^\circ$	$\phi=30^\circ$	$\phi=35^\circ$
La Marquesa Dam downstream	7.5	6.0	4.5
La Palma dam	10.0	9.2	8.5
Embankment of Kushiro river	4.5	3.8	2.8
Embankment of Rimnio river	14.0	12.0	10.0

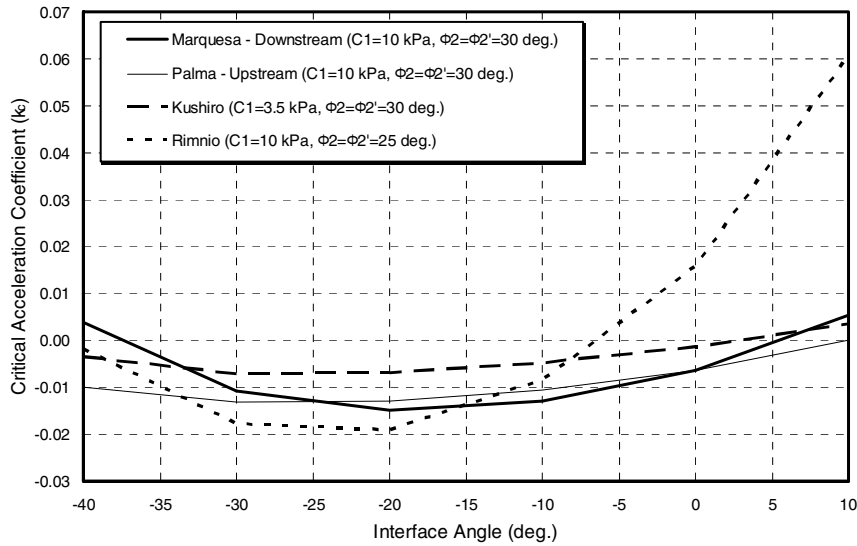


Fig. 5. Critical acceleration in terms of inclination of internal sub-plane.

5. THE UNDRAINED SOIL STRENGTH IN TERMS OF $N_{1(60)}$

Table 5 gives the measured $N_{1(60)}$ value of all slides analyzed. In addition, it compares (a) the back-estimated value of the undrained soil strength c_u of Fig. 3 with the range of values proposed by Seed and Harder (1990) for the measured $N_{1(60)}$ value, and (b) the back-estimated value of the ratio c_u/σ' of Fig. 3 with the lower bound proposed by Ishihara (1993) for the measured $N_{1(60)}$ of all slides analyzed. It can be observed that the pairs of $N_{1(60)}$ and the corresponding back-estimated c_u and c_u/σ' values are within the range proposed by Seed and Harder and the lower bound proposed by Ishihara. An exception is the Rimnio embankment where the back-estimated c_u is less than the proposed bounds by Seed and Harder.

In addition, the pairs show a more-or-less increase of c_u with $N_{1(60)}$. An exception is the La Palma Dam. Statistical analysis of the data is not performed, as the number of pairs is small.

6. CONCLUSIONS

In the paper, a two-body system model is extended to include both frictional and cohesive components of resistance. In this way, slides where the lower sub-plane of the slip surface is below the water level, and liquefies, but the upper part is above the water table and/or does not liquify can be simulated in a simplified manner. Then, the model is used to back-estimate the residual shear strength of four slides of small dams and embankments with the characteristics described above.

This study illustrated that the two-body model simulates with reasonable accuracy the kinematics of a number of liquefaction-induced slides. In addition, it illustrated that as soil displacement was primarily caused by static instability (due to earthquake-induced loss of strength), the applied accelerogram does not affect the results considerably. Finally, the pairs of the back-estimated c_u values and the corresponding $N_{1(60)}$ values are more-or-less within the range of values proposed by Seed and Harder (1990) and the lower bound proposed by Ishihara (1993).

Table 5. Measured $N_{1(60)}$ value of the Standard Penetration Test and corresponding (a) limits of c_u according to Seed and Harder (1990) and (b) the lower bound of c_u/σ'_v according to Ishihara (1993). Whether the back-estimated c_u value is within the limits and lower bound is assessed

Case	$N_{1(60)}$	Seed and Harder limits of c_u (kPa)	Is back-estimated c_u within the limits?	Ishihara lower bound of c_u/σ'_v	Is back-estimated c_u/σ'_v within the lower bound?
La Marquesa Dam downstream	9	2-21	Yes	0.04	Yes
La Palma dam	4	1-10	Yes	0	Yes
Embankment of Kushiro river	5	0-12	Yes	0	Yes
Embankment of Rimnio river	14	19-40	No	0.12	Yes

7. ACKNOWLEDGMENTS

This work was supported by the Hellenic Organization of Seismic Protection (OASP) during 2002 and 2003.

8. REFERENCES

1. European Prestandard. "Eurocode 8 - Design provisions of earthquake resistance of structures - Part 5: Foundations, retaining structures and geotechnical aspects", 1994.
2. Ishihara, K. "Liquefaction and Flow Failure During Earthquakes", 33rd Rankine Lecture, *Geotechnique* 43, No. 3, 1993, pp 351-415.
3. Kaneko M., Sasaki Y., Nishikawa J., Nagase M., Mamiya K.: "River Dike Failure in Japan by Earthquakes in 1993", Proceedings: Third International Conference on Recent Advances in Geotechnical Earthquake Engineering and Soil Dynamics, 1995, Vol I, pp 495-498.
4. Kerwin S. T., Stone J. J. "Liquefaction, failure and remediation: King Harbor Beach, California" *Journal of Geotechnical and Geoenvironmental Engineering*, 1997, Vol. 123, No. 8.
5. Kramer, S.L. "Geotechnical Earthquake Engineering", Prentice Hall, New Jersey, 1996.
6. ?ewmark, N. M. "Effect of earthquakes on dams and embankments", *Geotechnique*, Vol. 15, No. 2, London, England, June, 1965, pp. 139-160.
7. Olson S. M, Stark T. D., Walton W. H., Castro G "1907 static liquefaction flow failure of the Noth Dike of Wachusett Dam", *Journal of Geotechnical Engineering*, 2000, Vol. 126, No. 12.
8. Sarma S.K. "Stability analysis of embankments and slopes," *Journal of Geotechnical Engineering ASCE*; 1979, Vol.105, No. 12, pp. 1511-1524.
9. Sarma, S. K. and Chlimitzas G. Edited Report #2 for the project "Seismic Ground Displacements as a tool for town planning, design and mitigation", 2000.
10. Seed R. B. and Harder L. F. "SPT-based analysis of cyclic pore pressure and undrained residual strength". Proc. H. B. Seed Memorial Symp, Bi-Tech Publishing Ltd., Richmond, British Columbia, 1990, Vol 2, pp 351-376.
11. Seed H.B., Lee K. L., Idriss I. M., Makdisi F. I.: "The slides in the San Fernando Dams during the earthquake of February 9, 1971," *Journal of Geotechnical Engineering ASCE*, 1975, Vol. 101, No. 7, pp. 651-689.

12. Stamatopoulos C., Velgaki E. and Sarma S. "Sliding-block back analysis of earthquake-induced slides", *Soils and foundations*, The Japanese Geotechnical Society, 2000, Vol. 40, No. 6, pp 61-75.
13. Stamatopoulos C. "Collection-analysis of permanent seismic deformations and improvement of the seismic code", Final report, Hellenic Organization of aseismic propection (OASP), Athens, Greece, 2003.
14. Stamatopoulos C. and Aneroussis S. "Back analysis of the liquefaction failure at King Harbor Redondo Beach, California", Fifth International conference on case histories in Geotechnical Engineering, New York, NY, 2004, April 13-17 (in press).
15. Tika T.E. and Pitilakis K.D. "Liquefaction Induced Failure of a bridge embankment", Proceedings: Proceedings of the Second International Conference on Earthquake Geotechnical Engineering, Balkema, 199, pp. 631-636.